Journal of Autoimmunity 119 (2021) 102611

Contents lists available at ScienceDirect

Journal of Autoimmunity

journal homepage: www.elsevier.com/locate/jautimm

Short-chain fatty acid butyrate induces IL-10-producing B cells by regulating circadian-clock-related genes to ameliorate Sjögren's syndrome

Da Som Kim [a,b,c], Jin Seok Woo [a,b], Hong-Ki Min [d], Jeong-Won Choi [a,b], Jeong Hyeon Moon [a,b], Min-Jung Park [a,b], Seung-Ki Kwok [a,d], Sung-Hwan Park [a,d,**,1], Mi-La Cho [a,b,e,*,1]

[a] Rheumatism Research Center, Catholic Research Institute of Medical Science, College of Medicine, The Catholic University of Korea, Seoul, 06591, South Korea
[b] Laboratory of Immune Network, Catholic Research Institute of Medical Science, College of Medicine, College of Medicine, The Catholic University of Korea, Seoul, Republic of Korea
[c] Department of Biomedicine & Health Sciences, College of Medicine, The Catholic University of Korea, 222, Banpo-daero, Seocho-gu, Seoul, 06591, Republic of Korea
[d] Division of Rheumatology, Department of Internal Medicine, Seoul St. Mary's Hospital, College of Medicine, The Catholic University of Korea, Seoul, Republic of Korea
[e] Department of Medical Life Science, College of Medicine, The Catholic University of Korea, 222, Banpo-daero, Seocho-gu, Seoul, 06591, Republic of Korea

ARTICLE INFO

Keywords:
Sjögren's syndrome
Sodium butyrate
B cells

ABSTRACT

Objectives: Sjögren's syndrome (SS) is an autoimmune disease caused by inflammation of the exocrine gland. The pathological hallmark of SS is the infiltration of lymphocytes into the salivary glands. Increased infiltration of T and B cells into salivary glands exacerbates symptoms of SS. Several recent studies have identified the role of gut microbiota in SS. Butyrate, one of the metabolites of the gut microbiota, regulates T cells; however, its effects on B cells and SS remain unknown. This study determined the therapeutic effect of butyrate on regulating B cells in SS.

Methods: Various concentrations of butyrate were intraperitoneally injected three times per week in NOD/ShiLtJ (NOD) mice, the prototype animal model for SS, and observed for more than 10 weeks. Whole salivary flow rate and the histopathology of salivary glands were investigated. Human submandibular gland (HSG) cells and B cells in mouse spleen were used to confirm the anti-inflammatory and immunomodulatory effects of butyrate.

Results: Butyrate increased salivary flow rate in NOD mice and reduced inflammation of salivary gland tissues. It also regulated cell death and the expression of circadian-clock-related genes in HSG cells. Butyrate induced B cell regulation by increasing IL-10-producing B (B10) cells and decreasing IL-17-producing B cells, through the circadian clock genes RAR-related orphan receptor alpha and nuclear receptor subfamily 1 group D member 1.

Conclusion: The findings of this study imply that butyrate may ameliorate SS via reciprocal regulation of IL-10- and IL-17-producing B cells.

1. Introduction

Sjögren's syndrome (SS) is an autoimmune disease that affects the exocrine gland. The pathogenesis of SS is infiltration of immune cells into the salivary gland [1,2]. In SS, deregulated epithelial cells induce T-cell cytotoxicity and break B-cell tolerance. Recently, dysbiosis of the gut microbiome has been identified in SS and is considered a novel therapeutic target [3,4]. The butyrate-producer *Faecalibacterium* is reduced in the human gut microbiome of SS patients [5]. Butyrate is a short-chain fatty acid (SCFA) and a metabolite of the gut microbiome. Several bacteria are involved in the production of butyrate including *F. prausnitzii*, *Anaerostipes hadrus*, *Flintibacter butyricus*, and *Lactobacillus reuteri* [6–9]. *Akkermansia muciniphila* induces butyrate production from other butyrate-producing bacteria through a cross-feeding network [10]. *L. rhamnosus* is a bacterium that induces butyrate production through lactate [11]. Butyrate has a therapeutic effect on various autoimmune diseases by regulating T cells [12–15]. It also regulates plasma B cells [16,17] and increases interleukin 10 (IL-10)-producing B

* Corresponding author. Rheumatism Research Center, Catholic Research Institute of Medical Science, College of Medicine, The Catholic University of Korea, 222, Banpo-Daero, Seocho-gu, Seoul, 06591, Republic of Korea.
** Corresponding author. Division of Rheumatology, Department of Internal Medicine, Seoul St. Mary's Hospital, College of Medicine, The Catholic University of Korea, 222, Banpo-Daero, Seocho-gu, Seoul, 06591, Republic of Korea.
E-mail addresses: rapark@catholic.ac.kr (S.-H. Park), iammila@catholic.ac.kr (M.-L. Cho).
[1] These authors contributed equally to this work.

https://doi.org/10.1016/j.jaut.2021.102611
Received 7 October 2020; Received in revised form 26 January 2021; Accepted 27 January 2021
Available online 22 February 2021

(B10) cells [18–20]. Our previous study showed that butyrate modulates T cells and osteoclasts by inhibiting histone deacetylase (HDAC) to alleviate collagen-induced arthritis (CIA) [21]. However, HDAC is not regulated by butyrate in the B cells of NOD/ShiLtJ (NOD) mice, an SS animal model (data not shown), and thus is considered to have an HDAC-independent effect on B cells.

B10 cells are involved in the induction of regulatory T cells (Tregs) and have an anti-inflammatory role [22–24]. B cells can also express the IL-17 cytokine [25–27]. Although several mechanisms underlying cytokine secretion have been proposed, the majority are the subject of debate [28,29]. IL-10 and IL-17 are representative anti- and pro-inflammatory cytokines, respectively, so we focused on cytokine expression in B cells, which are important immune cells in SS pathogenesis.

The circadian clock is a biochemical oscillator that repeats every 24 h in most living things. It is regulated by circadian-clock-related genes and coordinates functions of the immune system. Nuclear receptor subfamily 1 group D member 1, also known as *NR1D1* or Rev-ErbA-Alpha, is a circadian-clock-related gene that is involved in T helper 17 cell (Th17) development through the circadian clock network and nuclear factor interleukin-3-regulated protein, also known as *NFIL3* or *E4BP4* [30]. Melatonin affects T-cell differentiation in multiple sclerosis by increasing type 1 regulatory T cells through RAR-related orphan receptor alpha (*RORα*) and inhibiting Th17 cells through *NR1D1* [31]. *RORα* and *NR1D1* bind directly to the IL-10 promoter and *NFIL3*, respectively. In addition, *NFIL3* can inhibit IL-12p40, which is essential for increasing Th17 cell responses via an IL-10-independent mechanism [32]. Circadian-clock-related genes are also associated with B-cell development [33,34] and human saliva flow rate [35]. In addition, the circadian clock is associated with gut microbiota [36–38] and its entrainment is induced by gut microbiota-derived metabolites [39].

In this study, we investigated the effects of butyrate on the balance of B cells via circadian-clock-related genes and its therapeutic effects on an experimental SS animal model.

2. Material and methods

2.1. Animals

NOD/ShiLtJ (NOD) and C57BL/6 mice were purchased from Jackson Laboratory (Bar Harbor, ME, USA) and Orient Bio Inc. (Gyeonggi-do, Korea), respectively. CD19-Cre mice were crossed with ROR$\alpha^{fl/fl}$ mice (University of Seoul, Korea) to facilitate *RORα* gene deletion in B cells. These mice were maintained in groups of five in polycarbonate cages in a specific-pathogen-free environment. They were provided access to standard mouse chow (Ralston Purina Co., St. Louis, MO, USA) and water *ad libitum*. All experimental procedures were approved by the Animal Research Ethics Committee at the Catholic University of Korea (Approval Nos. 2018-0178-06, 2018-0115-06, and 2019-0018-01).

2.2. Injection of L. rhamnosus

Ten-week-old NOD mice were orally administered 400 mg/kg of *L. rhamnosus* (CNS Pharm Korea Co., Ltd., Jincheon, Korea) daily in saline or saline alone. *L. rhamnosus* was administered after heat killing at 80 °C for 30 min.

2.3. Injection of sodium butyrate

Ten-week-old NOD mice were administered intraperitoneal injections of 1 g/kg sodium butyrate (Sigma, St. Louis, MO, USA) three times per week.

2.4. Measurement of salivary flow rate

The mice were anesthetized by isoflurane (2%) inhalation and injected intraperitoneally with pilocarpine (5 mg/kg; Sigma). Saliva was collected from the oral cavity 90 s later using a micropipette for 7 min in a microtube. The microtube containing the saliva was centrifuged, and the volume was measured using a micropipette. Salivary flow rate is expressed as μl/min/g.

2.5. Histological analysis

Histological analysis was performed to determine the extent of salivary gland inflammation. Salivary gland tissues from the mice were fixed in 4% paraformaldehyde, embedded in paraffin, and sectioned. Sections were stained with hematoxylin and eosin (H&E), examined under a photomicroscope (Olympus, Tokyo, Japan), and scored [40].

2.6. Immunohistochemistry

Immunohistochemistry was performed using a Vectastain ABC Kit (Vector Laboratories, Burlingame, CA, USA). Tissue sections were incubated overnight at 4 °C with primary antibodies against CD4, IL-17, and IL-21 (Abcam, Cambridge, UK); probed with a biotinylated secondary antibody; and stained with a streptavidin-peroxidase complex for 1 h. DAB chromogen (Dako, Carpinteria, CA, USA) was added as a substrate, and the samples were visualized by microscopy (Olympus). The positive cells were enumerated visually and the mean values were calculated.

2.7. Confocal microscopy

Tissue cryosections (7 μm thick) were fixed in methanol-acetone and stained with allophycocyanin (APC)-conjugated anti-B220, phycoerythrin (PE)-conjugated anti-IL-10, IL-17, RORα, NR1D1, and NFIL3 (eBioscience, San Diego, CA, USA). After overnight incubation at 4 °C, the stained sections were analyzed on a Zeiss microscope (LSM 510 Meta; Carl Zeiss, Oberkochen, Germany) at 200 × magnification.

2.8. Isolation and culture of salivary gland stem cells

Sphere-forming murine salivary gland stem cells (SGSCs) were isolated from mouse submandibular glands as previously described [41]. The thin fascia covering the submandibular glands was carefully removed to expose the submandibular tissues. The glands were washed three times in phosphate-buffered saline (PBS) containing 3% penicillin-streptomycin and chopped into small tissue fragments. The tissue fragments were kept at 37 °C in a 5% CO_2 atmosphere with Dulbecco's modified Eagle's medium (DMEM) containing 1 mg/mL collagenase I (Worthington Biochemical Products, Lakewood, NJ, USA) for 30 min. Then the fragments were centrifuged and the cell pellet was resuspended in DMEM. The cells were filtered through a 40-μm cell strainer (BD Biosciences, Franklin Lakes, NJ, USA) into a single-cell suspension. After centrifugation, the cells were cultured in DMEM/F12 (1:1 mixture, v/v; Gibco, Grand Island, NY, USA) supplemented with 20 ng/mL: epidermal growth factor (Peprotech, Rocky Hill, NJ, USA), 20 ng/mL fibroblast growth factor-2 (Peprotech), 1% N2 supplement (Gibco), 1% insulin-transferrin-selenium (Gibco), 1 μm dexamethasone (Sigma), and 1% penicillin-streptomycin (Sigma). SGCSs were cultured in Matrigel™ (Corning Costar, Cambridge, MA, USA). Salisphere formation was observed after 2–3 days in culture, and continued to grow in size over 10 days in culture.

2.9. Salivary gland cell isolation

Murine salivary gland tissues were minced in 1 unit/mL dispase solution (Stemcell Technologies, Vancouver, British Columbia, Canada) containing 2 mg/mL collagenase IV (Gibco) and were then incubated at 37 °C until re-suspension was possible. After centrifugation, the cells were filtered through a 40-μm cell strainer (BD Biosciences) into a

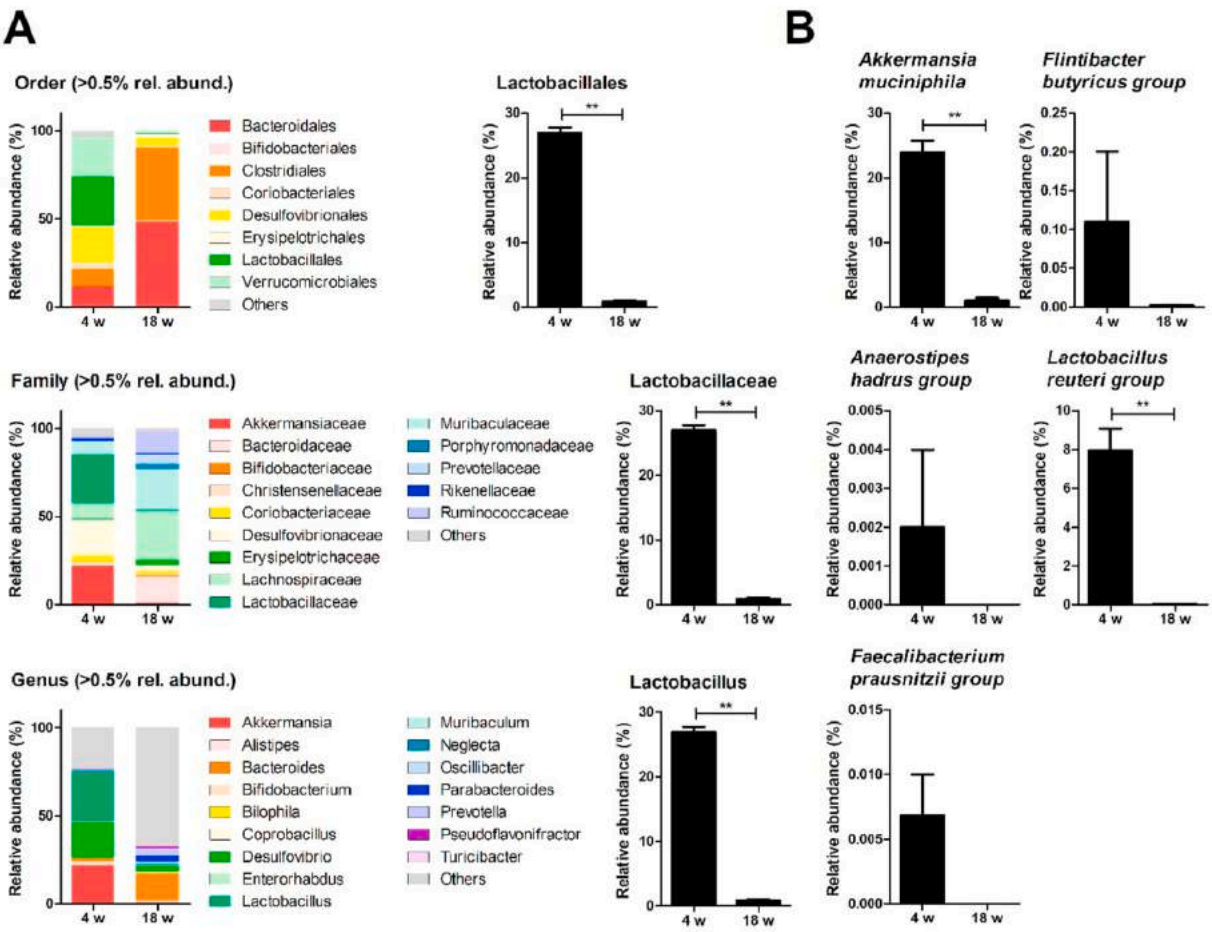

Fig. 1. Butyrate-producing bacteria were reduced in NOD mice. (A) Composition of cecal microbiota at the order, family, and genus level of 4- and 18-week-old NOD mice (n = 5). W: weeks of age. Relative abundance of *Lactobacillales*, *Lactobacillaceae*, and *Lactobacillus* is shown. (B) Bacteria that are directly or indirectly involved in butyrate production at the species level of 4- and 18-week-old NOD mice (n = 5). Two-tailed unpaired *t*-test was used for statistical analysis. **p < 0.01.

single-cell suspension.

2.10. Flow cytometry

Human submandibular gland (HSG) cells were immunostained using an Annexin V-FITC Apoptosis Kit (BioVision, Inc., Milpitas, CA). Splenocytes and salivary gland cells were stained with PerCP-Cy5.5-conjugated anti-CD19, fluorescein isothiocyanate-conjugated anti-CD5, PE-conjugated anti-CD1d and IL-17, APC-conjugated anti-IL-10 (eBioscience), and primary antibody against RORα (Santa Cruz, Texas, USA), followed by probing with an APC-conjugated secondary antibody (SouthernBiotech, Birmingham, AL, USA). For intracellular staining, cells were restimulated with 25 ng/ml phorbol 12-myristate 13-acetate and 250 ng/mL ionomycin (Sigma) for 4 h in the presence of GolgiStop (BD Biosciences). The data were analyzed using FlowJo software (Tree Star, Ashland, OR, USA).

2.11. Western blot analysis

The protein levels of caspase 1, caspase 3, caspase 8, RORα, NR1D1, GAPDH (Abcam), mixed lineage kinase domain-like protein (MLKL) (Merck Millipore, Danvers, MD, USA), receptor-interacting serine/threonine-protein kinase 3 (RIPK3), β-actin (Santa Cruz), and NFIL3 (Cell Signaling, Danvers, MA, USA) were measured using a Western blot system (SNAP i.d. Protein Detection System; Merck Millipore, Darmstadt, Germany). Protein concentrations of the cell lysates were determined using the Bradford method (Bio-Rad, Hercules, CA, USA), and samples were separated on a sodium dodecyl sulfate polyacrylamide gel and electrotransferred to a nitrocellulose membrane (Amersham Pharmacia, Uppsala, Sweden). The membrane was incubated with primary antibodies diluted in 0.1% skim milk in Tris-buffered saline and incubated for 20 min at room temperature. The membrane was washed and incubated with a horseradish peroxidase-conjugated secondary antibody for 20 min at room temperature. Hybridized bands were detected using an enhanced chemiluminescence detection kit (Pierce, Rockford, IL, USA) and Hyperfilm (Agfa, Mortsel, Belgium).

2.12. Real-time polymerase chain reaction

The mRNA was extracted using TRI Reagent (Molecular Research Center, Inc., Cincinnati, OH, USA) according to the manufacturer's instructions. cDNA was synthesized using a Super Script Reverse Transcription system (TaKaRa, Shiga, Japan). A Light-Cycler 2.0 instrument (software version 4.0; Roche Diagnostics, Indianapolis, IN, USA) was used for PCR amplification. All reactions were performed using Light-Cycler FastStart DNA Master SYBR Green I Mix (TaKaRa) following the manufacturer's instructions. The following primers were used: BMAL1, 5′-TCA-GTG-ATT-TCA-TGT-CCC-CG-3' (sense) and 5′-AGG-GTC-ATC-TTT-GTC-TGT-GTC-3' (antisense); Cry1, 5′-TCC-CGT-CTG-TTT-GTG-ATT-CG-3' (sense) and 5′-TTA-ATA-GCT-GCG-TCT-CGT-TCC-3' (antisense); IL-10, 5′-GGC-CCA-GAA-ATC-AAG-GAG-CA-3' (sense) and 5′-AGA-AAT-CGA-TGA-CAG-CGC-CT-3' (antisense); IL-17, 5′-CCT-CAA-AGC-TCA-GCG-TGT-CC-3' (sense) and 5′-GAG-CTC-ACT-TTT-GCG-CCA-AG-3' (antisense); RORα, 5′-GGA-AGG-TCT-GCC-ACG-TTA-TCT-G-

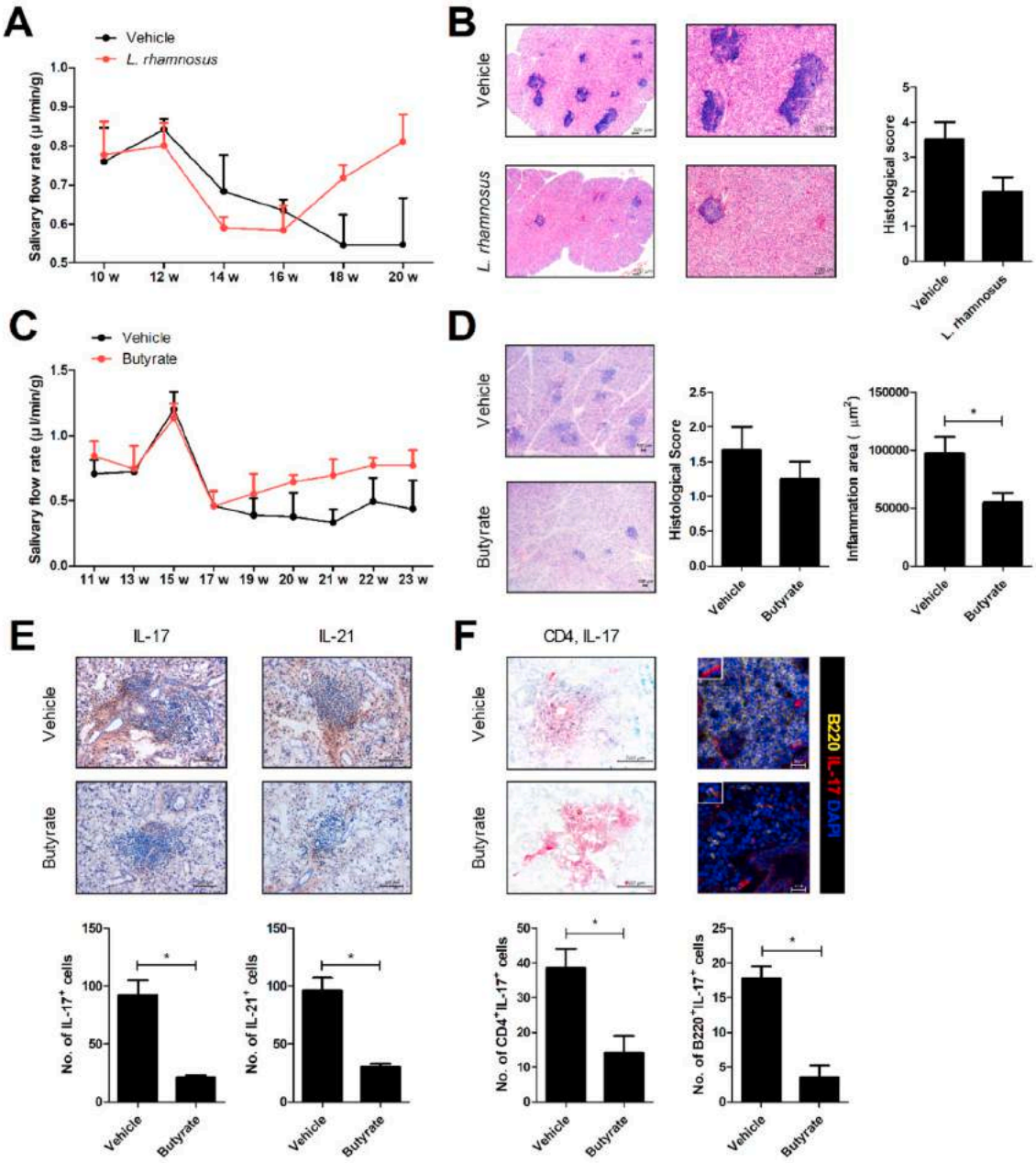

Fig. 2. Butyrate-producing bacteria and butyrate have therapeutic effects on a mouse model of SS and regulates SGSCs differentiation. (A) Ten-week-old NOD mice (n = 5) were treated with 400 mg/kg L. *rhamnosus* or vehicle alone via daily oral feeding. Salivary flow rate graph measured every 2 weeks. (B) Histological staining of salivary gland tissue sections with hematoxylin and eosin (original magnification, 40×). Histological inflammation scores are shown (n = 5). (C) Eleven-week-old NOD mice (n = 5) were treated with 1 g/kg butyrate or vehicle alone by intraperitoneal administration three times a week. Mice were observed for 12 weeks and salivary flow rate was measured every 2 weeks. (D) Histological staining of salivary gland tissue sections with hematoxylin and eosin (original magnification, 40×). Histological inflammation scores are shown (n = 5). (E) Representative histological features of the salivary glands of vehicle- and butyrate-treated mice (n = 5). Immunohistochemical staining for IL-17 and IL-21 (original magnification, 200×) were shown. Graph shows the numbers of cells expressing IL-17 and IL-21. (F) Representative histological features of the salivary glands of vehicle- and butyrate-treated mice (n = 5). Immunohistochemical staining for CD4 and IL-17 or confocal microscopy for B220 and IL-17 (original magnification, 400×) were shown. Graph shows the numbers of cells CD4 and IL-17 or B220 and IL-17 co-stained cells. CD4, red; IL-17, blue; overlap, purple (left panel). Two-tailed unpaired *t*-test was used for statistical analyses. Data are representative of three independent experiments. *$p < 0.05$.

3' (sense) and 5′-TCC-AAA-TCC-CAC-CTG-GAA-AC-3' (antisense); NR1D1, 5′-GCC-ATG-TTT-GAC-TTC-AGC-G-3' (sense) and 5′-AAT-TCT-CCA-TTC-CCG-AGC-G-3' (antisense); NFIL3, 5′-GGT-TTC-CGA-AGC-TGA-GAA-TTT-G-3' (sense) and 5′-CCA-TGC-ATA-GCT-CGG-TCA-G-3' (antisense); mouse β-actin, 5′-GAA-ATC-GTG-CGT-GAC-ATC-AAA-G-3' (sense) and 5′-TGT-AGT-TTC-ATG-GAT-GCC-ACA-G-3' (antisense); and human β-actin, 5′-GGA-CTT-CGA-GCA-AGA-GAT-GG-3' (sense) and 5′-TGT-GTT-GGG-GTA-CAG-GTC-TTT-G-3' (antisense). All mRNA levels were normalized to β-actin.

2.13. Enzyme-linked immunosorbent assay

The amounts of IL-10 in the cultured supernatants from mouse cells were measured by sandwich enzyme-linked immunoassay (ELISA) (R&D Systems, Minneapolis, MN, USA). Horseradish peroxidase-avidin (R&D Systems) was used for color development. The amounts of

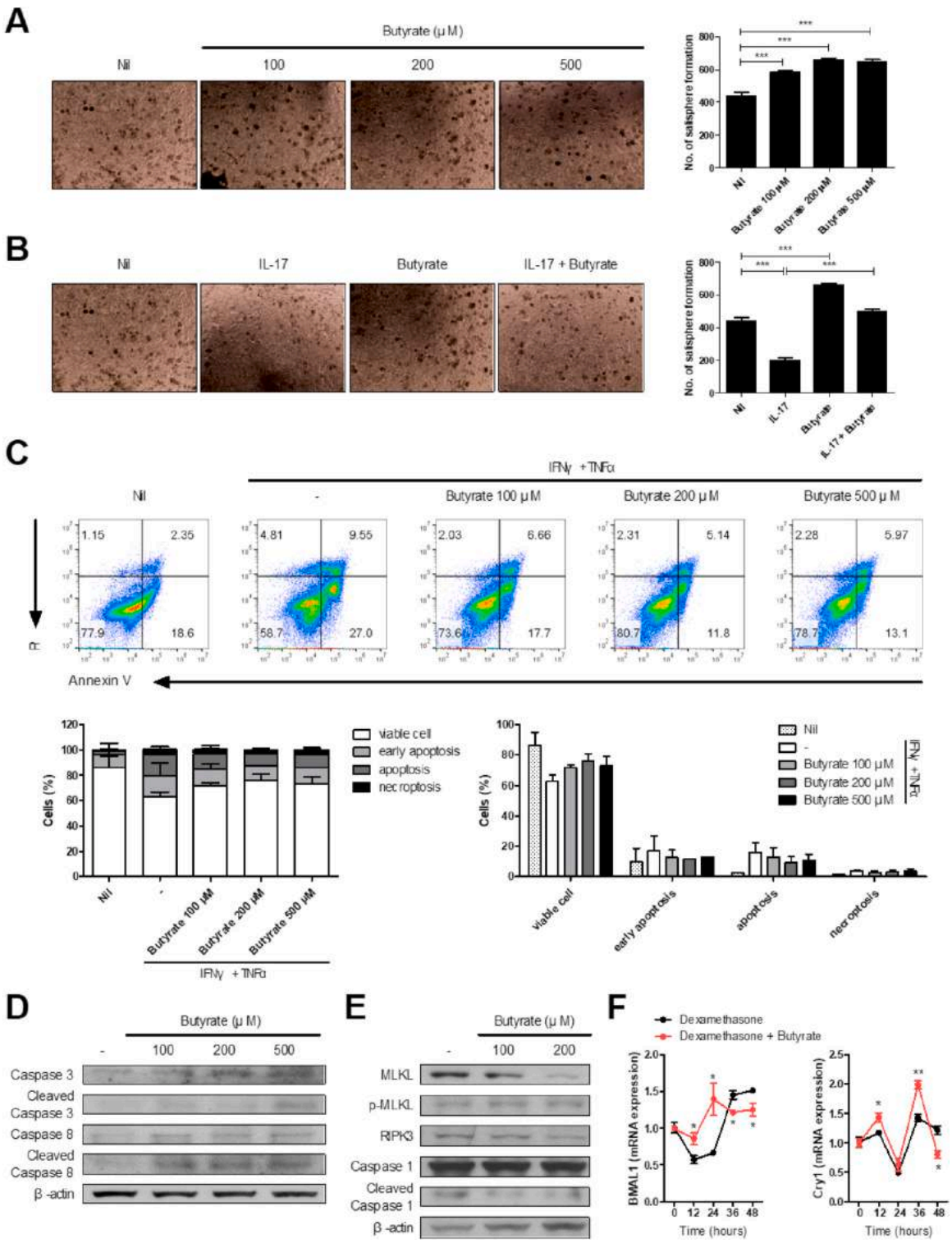

Fig. 3. Butyrate regulates development of SGSCs and cell death and circadian rhythm of HSG cells. (A) SGSCs were isolated and cultured in the presence or absence of 100, 200, and 500 μM butyrate. Representative photographs are shown. The numbers of salispheres are shown. (B) SGSCs were isolated and cultured in the presence or absence of 20 ng/mL IL-17 and 200 μM butyrate. Representative photographs are shown. The numbers of salispheres are shown. (C) HSG cells were stimulated with 10 ng/mL of IFNγ and 50 ng/mL of TNFα, and stained with PI and Annexin V. The percentage of cells in each region is shown (PI^-annexin V^-, viable cell; PI^-annexin V^+, early apoptosis; PI^+annexin V^+, apoptosis; PI^+annexin V^-, necroptosis). (D) HSG cells were cultured with 10 ng/mL IFNγ and 50 ng/mL TNFα in the presence or absence of 100, 200, and 500 μM butyrate. The cells were prepared for determination of apoptosis marker expression. (E) HSG cells were cultured with 10 ng/mL IFNγ and 50 ng/mL TNFα in the presence or absence of 100 and 200 μM butyrate. The cells were prepared for determination of inflammatory cell death marker expression. (F) HSG cell lines were cultured with 100 nM dexamethasone in the presence or absence of butyrate. The cells were harvested at 12-h intervals and mRNA levels of circadian clock related genes were measured. A two-tailed unpaired *t*-test was used for statistical analysis. Data are representative of three independent experiments. *$p < 0.05$, **$p < 0.01$, ***$p < 0.001$.

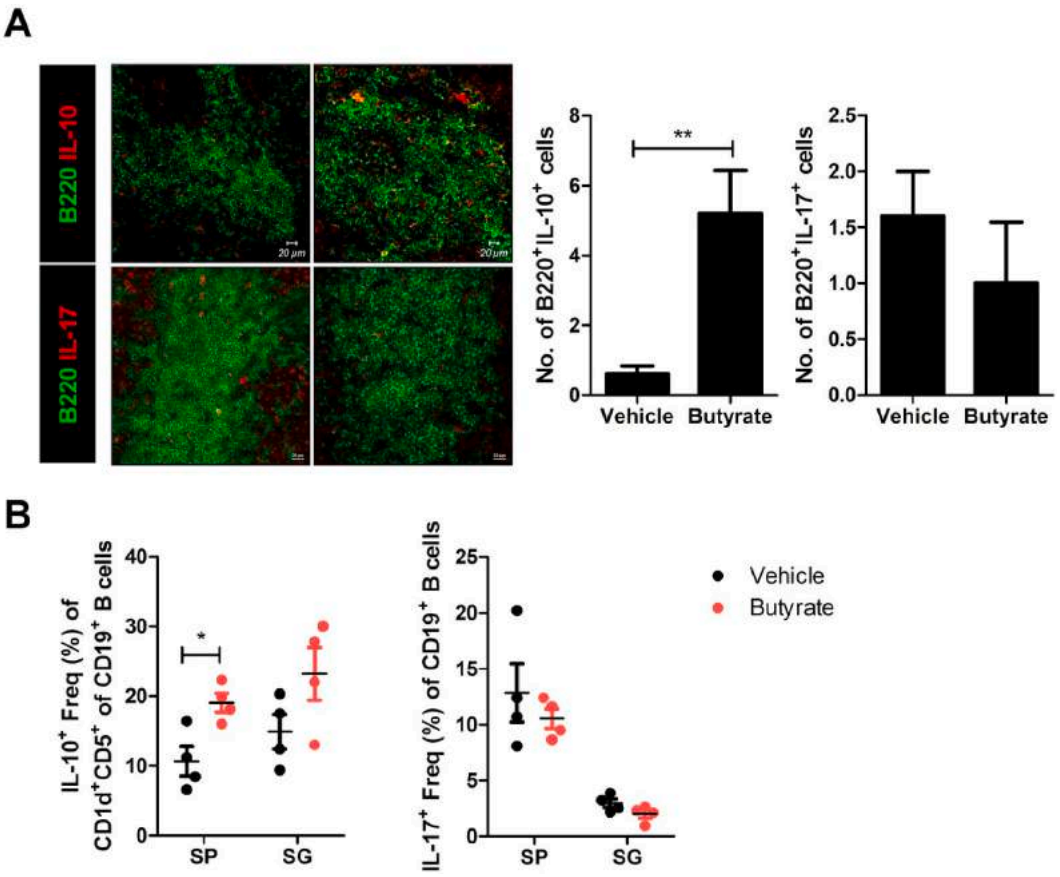

Fig. 4. Butyrate regulates B cells in a NOD mouse model of SS *ex vivo*. (A) Confocal microscopy of spleen cryosections of vehicle- and butyrate 1 g/kg-treated NOD mice, stained for B220 and IL-10 (IL-10-producing B cells, B10 cells) or B220 and IL-17 (IL-17-producing B cells) (original magnification, 200×). The numbers of positive cells are shown (n = 5). (B) Flow cytometry analysis of the B10 and IL-17-producing B cell populations in splenocytes or salivary gland cells from vehicle- and butyrate-treated NOD mice. Two-tailed unpaired *t*-test and one-way ANOVA were used for statistical analysis. Data are representative of three independent experiments. *p < 0.05, **p < 0.01.

immunoglobulin G (IgG) were measured using ELISA kits (Bethyl Laboratories, Montgomery, TX, USA). The absorbance was determined on an ELISA microplate reader (Molecular Devices, Sunnyvale, CA, USA).

2.14. Small interfering RNA transfection

Small interfering RNA (siRNA) for NFIL3 was acquired from Cosmo Genetech (Seoul, Korea). Before transfection, murine B cells were cultured with lipopolysaccharide (LPS) from *Escherichia coli* O111:B4 (LPS, 100 ng/mL; Sigma). One day later, cells were transfected using the Amaxa 4D-nucleofector X unit according to the manufacturer's recommendations with a primary cell kit (Lonza, Cologne, Germany).

3. Results

3.1. Butyrate-producing bacteria were decreased in NOD mice

NOD mice are representative murine models of SS and generally tend to spontaneously develop inflammatory lesions in the salivary gland at 10 weeks old [42]. Therefore, we used cecal from 4- and 18-week-old mice to compare changes in gut microbiota according to disease onset. The gut microbiota composition was significantly changed regarding the order, family, and genus levels. In particular, *Lactobacillus* and its higher classifications were significantly decreased at the onset of SS (Fig. 1A). Butyrate-producing bacteria were also reduced (Fig. 1B).

3.2. Butyrate-producing bacteria and butyrate alleviates SS and regulates the inflammation of salivary gland tissue

To investigate the therapeutic effect of butyrate, NOD mice were treated with butyrate-producing bacteria, *L. rhamnosus*. Administration of *L. rhamnosus* to NOD mice increased the salivary flow rate compared to vehicle (Fig. 2A) and alleviated inflammation in salivary gland tissues (Fig. 2B). Also, salivary flow rates were increased by butyrate compared to vehicle treatment (Fig. 2C). Histological evaluation of salivary gland tissues showed that histological scores and inflamed areas were reduced in butyrate-treated mice compared to vehicle-treated mice (Fig. 2D). Infiltration of IL-17- and IL-21-producing cells into salivary glands was decreased in butyrate-treated NOD mice (Fig. 2E). The expression of IL-17 in T and B cells were also reduced by butyrate treatment (Fig. 2F). These results show that butyrate is effective in attenuating SS.

3.3. Butyrate regulates differentiation of SGECs and cell death and circadian-clock-related genes in HSG cells

To confirmed effect of butyrate in salivary gland related cells, sphere-forming efficiency was conducted in the SGCSs. SGSCs cultured with butyrate had increased salisphere-forming efficiency (Fig. 3A). The salisphere-forming ability was disrupted by the addition of IL-17, and was restored by the addition of IL-17 together with butyrate (Fig. 3B). Cell death markers are differentially expressed in the salivary gland of SS patients and healthy individuals [43]. In this study, interferon gamma (IFNγ) and tumor necrosis factor alpha (TNFα) induced cell death in HSG cells, which was rescued by butyrate (Fig. 3C). The apoptotic markers

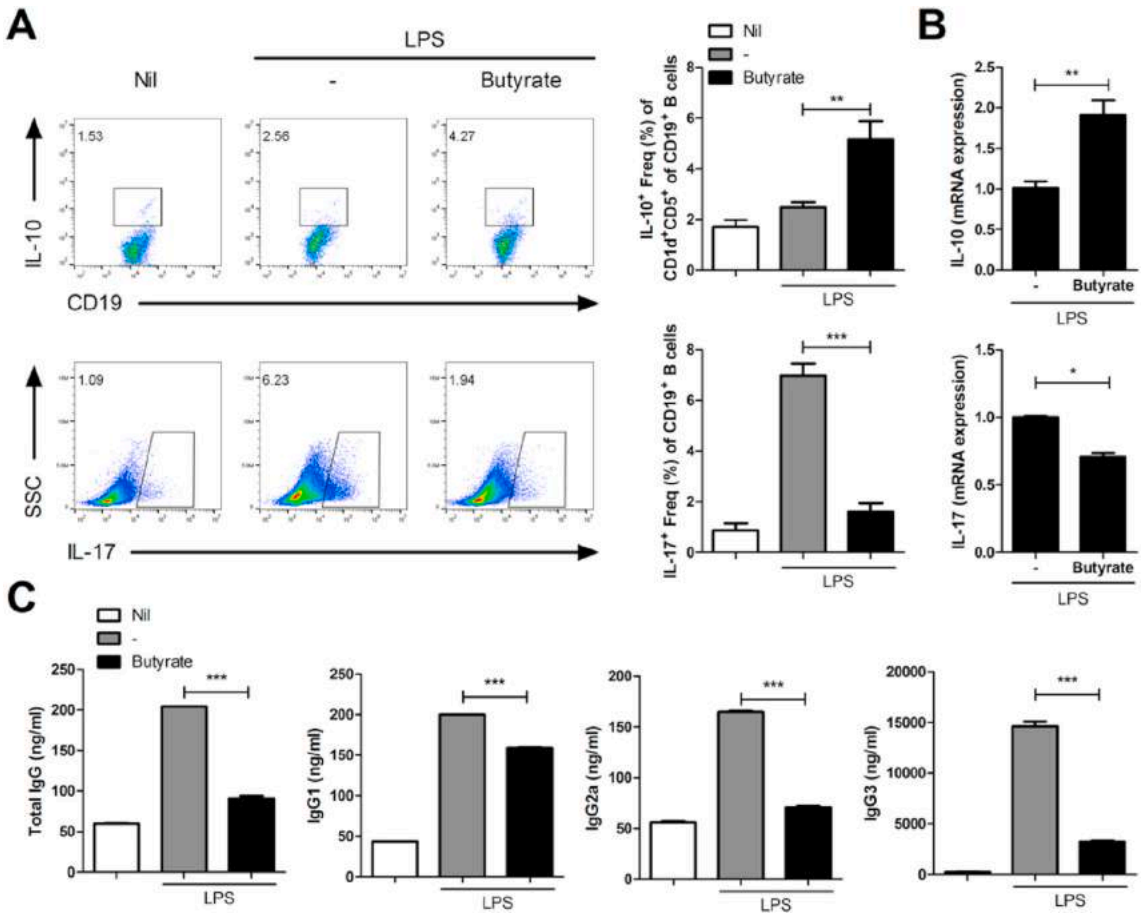

Fig. 5. Butyrate regulates B cells in a NOD mouse model of *SS in vitro*. $CD19^+$ B cells were extracted from the spleens of NOD mice, cultured with butyrate under LPS conditions. Cells were cultured for 24 h (B) or 72 h (A and C). (A) The cells were subjected to flow cytometry analysis of IL-10- or IL-17-expressing B cells. Percentages of IL-10- or IL-17-positive cells are shown. (B) Relative mRNA expression of IL-10 and IL-17 was analyzed by real-time PCR. (C) Total IgG, IgG1, IgG2a, and IgG3 were evaluated by ELISA using culture supernatants. Two-tailed unpaired *t*-test and one-way ANOVA were used for statistical analysis. Data are representative of three independent experiments. *$p < 0.05$, **$p < 0.01$, ***$p < 0.001$.

caspase 3 and caspase 8, and markers of inflammaroty cell death, MLKL, RIPK3, and caspase 1 were increased and decreased in butyrate-treated cells, respectively (Fig. 3D and E), confirming that necroptosis is converted to apoptosis by butyrate. SCFAs induce circadian-clock entrainment [39], and treatment of HSG cells with dexamethasone can induce the circadian rhythm [44]. In this study, HSG cells were treated with dexamethasone to confirm circadian-clock-related gene expression; brain and muscle ARNT-like 1 (*BMAL1*) decreased at 12 h and peaked at 48 h, and crystallin lambda 1 (*Cry1*) peaked at 12 and 36 h and decreased at 24 h. After butyrate treatment, the cycling pattern of *BMAL1* was altered, and *Cry1* levels increased significantly (Fig. 3F). These results show that butyrate can regulate circadian-clock-related genes in HSG cells.

3.4. Butyrate regulates the B cells of NOD mouse ex vivo

We investigated the role of butyrate in the production of IL-10 and IL-17 in B cells. The butyrate-treated group had increased levels of B10 cells and decreased levels of IL-17-producing B cells compared to the vehicle-treated group (Fig. 4A). The regulation of B10 and IL-17-producing B cells in the splenocytes and salivary gland cells of the NOD mice was analyzed by flow cytometry, which showed that the B10 cells of the splenocytes were significantly increased by butyrate (Fig. 4B). These data imply that butyrate can simultaneously regulate B10 and IL-17-producing B cells.

3.5. Butyrate regulates B cells of NOD mouse in in vitro

B cells were isolated from the spleen of NOD mice and cultured for 3 days with or without butyrate under LPS conditions. B10 cells and IL-17-producing B cells were increased and reduced in butyrate-treated cells, respectively (Fig. 5A). Also, the mRNA levels of IL-10 and IL-17 were regulated by butyrate (Fig. 5B). Total IgG, IgG1, IgG2a, and IgG3 levels were reduced in the supernatant of butyrate-treated B cells (Fig. 5C).

3.6. Butyrate increases B10 cells through RORα

We investigated the role of *RORα* in the regulation of B10 cells by butyrate. *RORα*-expressing B cells were increased in the salivary gland tissues of butyrate-treated NOD mice (Fig. 6A). B cells from mouse splenocytes were cultured under LPS conditions, and the expression level of *RORα* was increased by butyrate (Fig. 6B–D). The effect of butyrate on increasing B10 was inhibited by the *RORα* antagonist SR3335 (Fig. 6E). $ROR\alpha^{fl/fl}$ mice were bred with CD19-Cre mice to obtain B-cell-specific deletion of *RORα* (Fig. 6F). B cells were isolated from WT (C57BL/6) and $ROR\alpha^{fl/fl}$/CD19-Cre mice. In *RORα*-deleted B cells, the population of B10 cells was reduced (Fig. 6G and H). After culturing under LPS conditions for 3 days, the B10 population and IL-10 cytokine expression did not increase even with butyrate treatment (Fig. 6I and J). Collectively, these data imply that changes in the B10 cell population by butyrate are regulated by *RORα*.

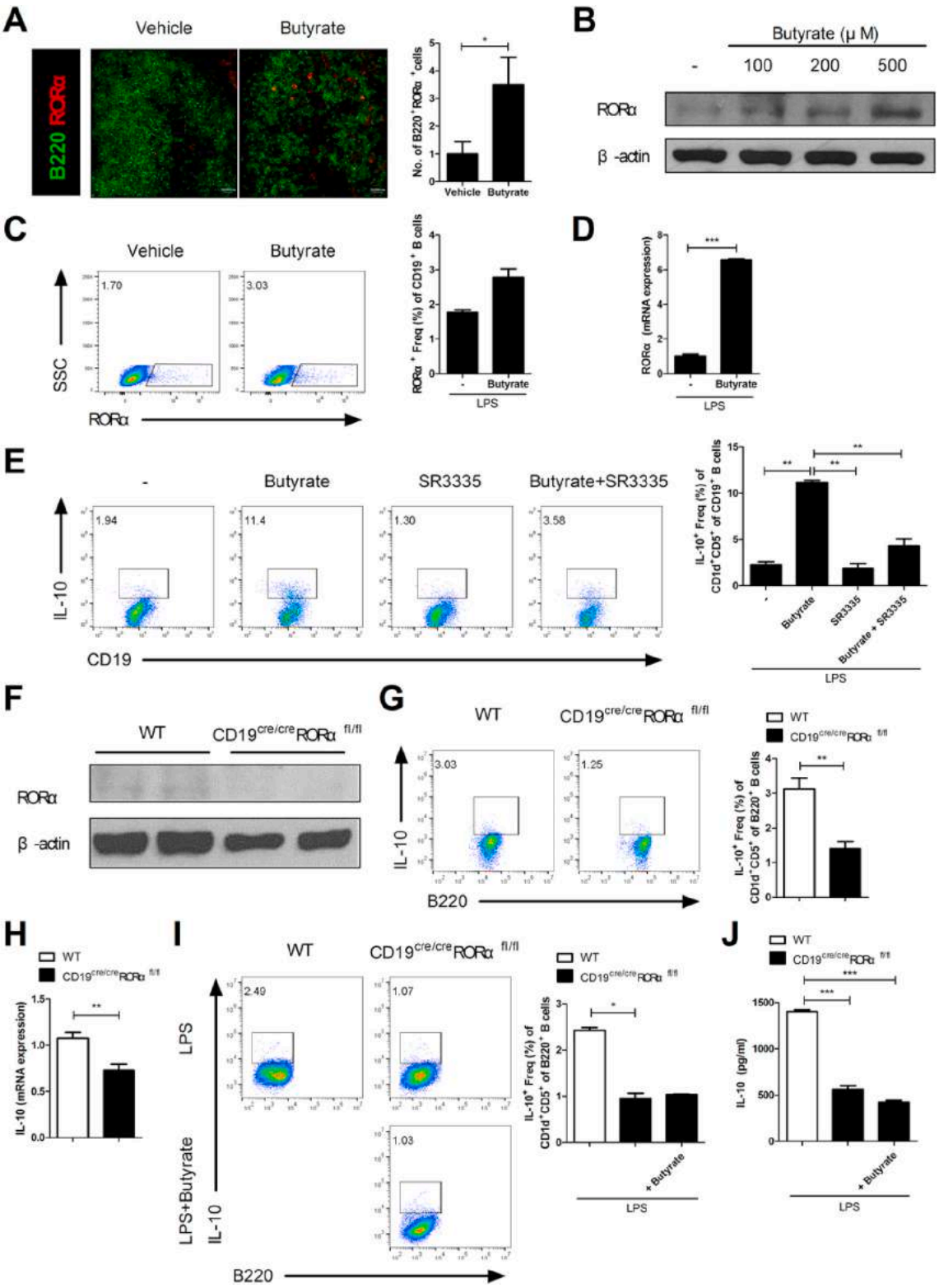

Fig. 6. Butyrate increases B10 cells through *RORα*. (A) Confocal microscopy of salivary gland cryosections of vehicle- and butyrate 1 g/kg-treated NOD mice, stained for B220 and *RORα* (original magnification, 200×). (B–E) $CD19^+$ B cells were sorted from the C57BL/6 mice, cultured with butyrate and/or SR3335 under LPS conditions. Cells were cultured for 24 h (D) or 72 h (B, C, and E). (B) Western blotting was performed for *RORα* expression. (C) Flow cytometry analysis of *RORα*-producing B cell populations. (D) Relative mRNA expression of *RORα*. (E) The cells were subjected to flow cytometry analysis of B10 cells. Percentages of IL-10-positive cells are shown. (F) Western blot of spleen protein displays WT and B-cell-specific *RORα*-deficient mouse expression of *RORα*. (G) and (H), $B220^+$ B cells were isolated from splenocytes, followed by flow cytometry analysis (G) and real-time PCR (H). (I and J), $B220^+$ B cells were isolated from splenocytes and cultured with butyrate under LPS conditions for 72 h, and flow cytometry analysis (I) and ELISA (J) were performed. A two-tailed unpaired *t*-test and one-way ANOVA were used for statistical analysis. Data are representative of three independent experiments. *$p < 0.05$, **$p < 0.01$, ***$p < 0.001$.

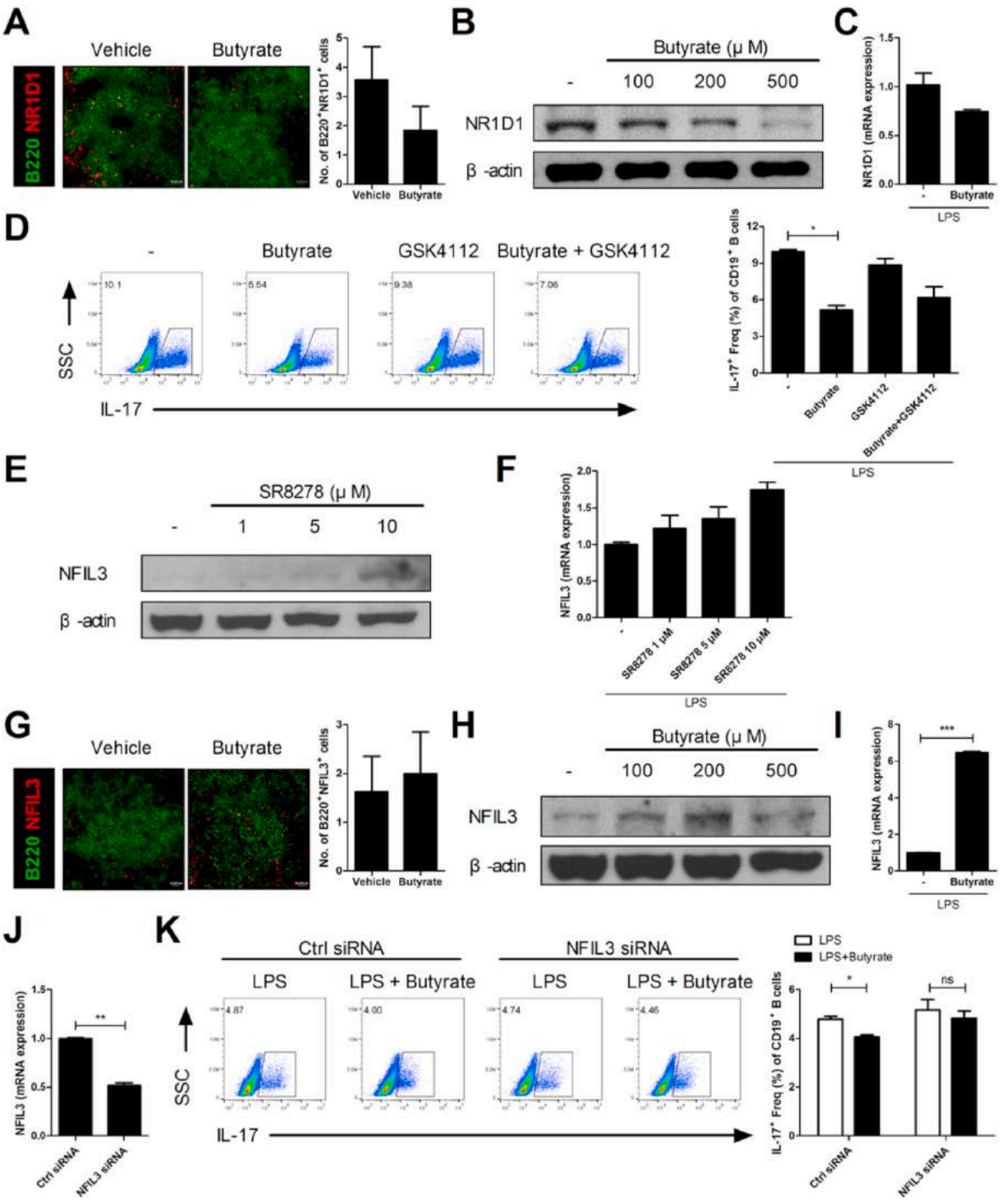

Fig. 7. Butyrate reduces IL-17-producing B cells through *NR1D1* and *NFIL3*. (A), Confocal microscopy of salivary gland cryosections of vehicle- and butyrate 1 g/kg-treated NOD mice, stained for B220 and *NR1D1* (original magnification, 200×). (B-F) and (H–K), $CD19^+$ B cells were isolated from the C57BL/6 mice, cultured with butyrate and/or GSK4112 and SR8278 under LPS conditions. Cells were cultured for 24 h (C, F, and I) or 72 h (B, D, E, and H). (B), Western blot was performed for *NR1D1* expression. (C) Relative mRNA expression of *NR1D1*. (D) Flow cytometry analysis of the IL-17-producing B cells. Percentage of IL-17-positive cells are shown. (E) Western blotting was performed for *NFIL3* expression. (F) Relative mRNA expression of *NFIL3*. (G) Confocal microscopy of salivary gland cryosections of vehicle- and butyrate 1 g/kg-treated NOD mice, stained for B220 and *NFIL3* (original magnification, 200×). (H) Western blot shows expression of *NFIL3*. (I) Relative mRNA expression of *NFIL3*. (J) Relative mRNA expression of *NFIL3* after NFIL3 siRNA treatment. (K) Percentage of IL-17-producing B cells after *NFIL3* siRNA treatment. Two-tailed unpaired *t*-test and one-way ANOVA were used for statistical analysis. Data are representative of three independent experiments. *$p < 0.05$, **$p < 0.01$, ***$p < 0.001$.

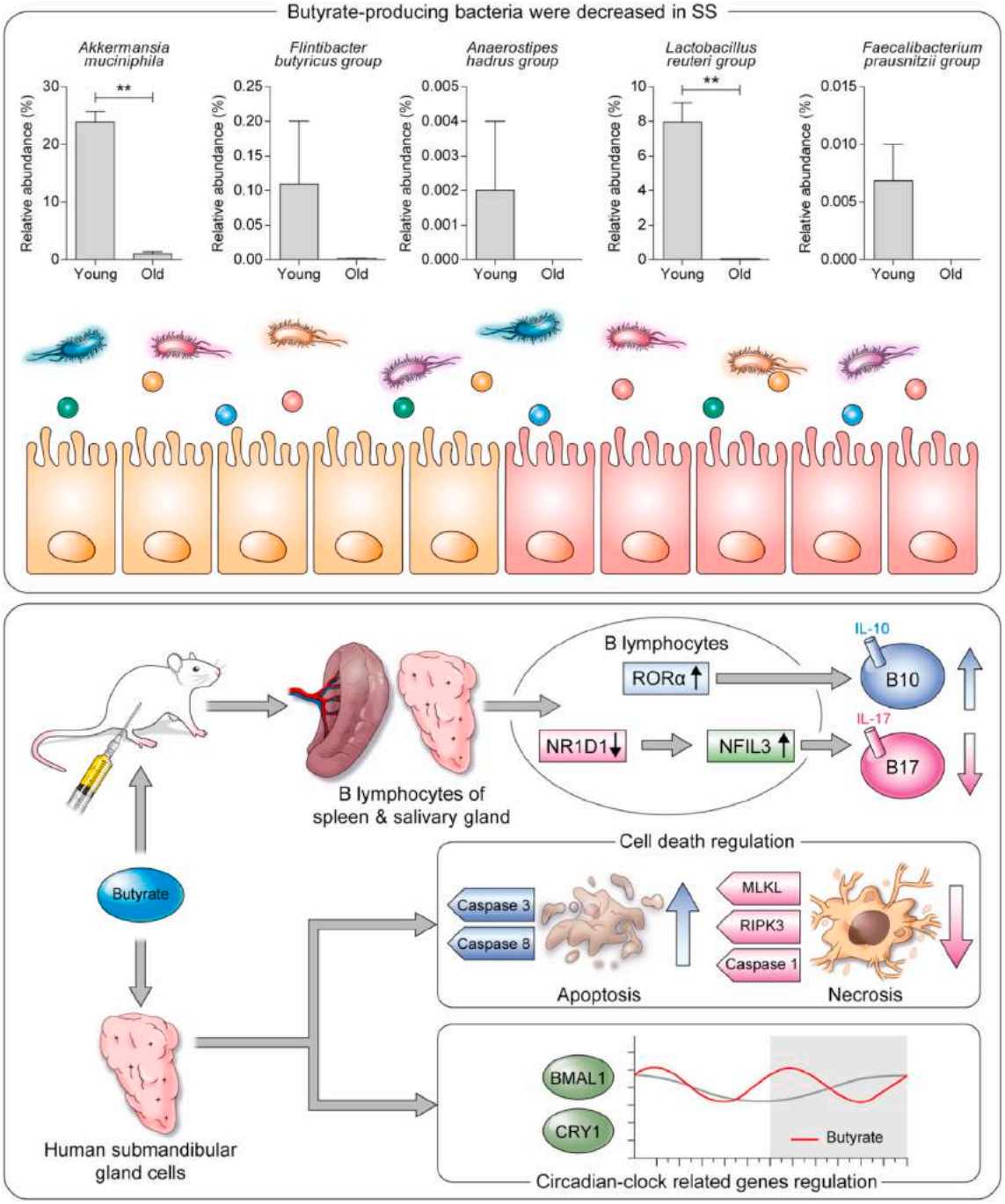

Fig. 8. Potential therapeutic effects of butyrate in Sjögren's syndrome.

3.7. Butyrate reduces IL-17-producing B cells through NR1D1 and NFIL3

We investigated the role of butyrate in IL-17-producing B cells. *NR1D1* was reduced in the salivary gland tissues of butyrate-treated NOD mice (Fig. 7A), and butyrate decreased its expression level in cultured B cells (Fig. 7B and C). IL-17-producing B cells were not inhibited by treatment with the *NR1D1* agonist GSK4112 (Fig. 7D), and *NFIL3* was increased by the *NR1D1* antagonist SR8278 (Fig. 7E and F). *NFIL3* showed an increasing trend in the salivary gland of butyrate-treated mice (Fig. 7G), and was increased by stimulating with butyrate (Fig. 7H and I). To confirm the direct regulation of butyrate, an experiment was performed in which B cells were transfected with *NFIL3* siRNA (Fig. 7J). As a result, the IL-17-producing B cells were not reduced with *NFIL3* siRNA, even with the addition of butyrate (Fig. 7K). Taken together, butyrate inhibited IL-17-producing B cells through a pathway that reduced *NR1D1* and increased *NFIL3*. To confirm that circadian-clock-related genes regulated the effect of butyrate, B cells were treated with CGP52608, an agonist of *RORα*, and SR8278, an inhibitor of *NR1D1*, and compared with butyrate. The combination treatment of CGP52608 and SR8278 showed a weaker effect than butyrate, but B10 tended to increase and B17 decreased (Supplementary Figs. 1A and B) (see Fig. 8).

4. Discussion

Microorganisms exist in various sites including the gastrointestinal tract (gut microbiota) and nasal cavities (oral microbiota) [45]. Recently, gut microbiota have been analyzed in various autoimmune

diseases. Although gut dysbiosis has been confirmed in SS, treatment strategies using microbiota or microbiota-derived metabolites are insufficient. We conducted gut microbiota analysis before and after the onset of SS in NOD mice and confirmed that the distribution of gut microbiota changed. In a previous study that analyzed the microbiota in a dessicating stress-induced SS mouse model, *Lactobacillus*, *Alistipes*, and *Desulfovibrio* were equally decreased [5]. Our data showed that bacteria, which included *Lactobacillus*, were decreased in aged NOD mice compared to young mice, and administration of *L. rhamnosus* attenuated the severity of SS.

A recent study demonstrated that butyrate regulated the Th17/Treg balance in a mouse model of rheumatoid arthritis (RA) [21]. Although several studies have reported gut dysbiosis in SS, the role of bacteria or metabolites in SS is unknown. In this study, we investigated the therapeutic effect of butyrate produced by bacteria in NOD mice with SS. Administration of butyrate resulted in an increased salivary flow rate and decreased infiltration of inflammatory cells into the salivary glands compared to vehicle-treated mice. Furthermore, butyrate increased salisphere formation in SGSCs. In addition, treatment with butyrate prevented cell death, which is induced by IFNγ and TNFα. Apoptosis is the final outcome of SS. These data imply that the butyrate produced by bacteria is crucial to SS development and have therapeutic potential.

Cellular and molecular pathways are important in SS pathogenesis, and B cells act as outcomes in this process [2]. In fact, abnormality of B cells is displayed in SS patients, but further studies are needed to evaluate disease activity by controlling the balance of B cells. In this study, the therapeutic effect was confirmed in NOD mice by controlling B cells using butyrate.

B10 cells are involved in the induction of regulatory T cells and expression is regulated by *RORα* [22,31]. A recent study showed that B10 cells and IL-17-producing T cells regulate CIA [46]. The number of B10 cells was increased in the spleen of butyrate-treated mice compared to vehicle-treated mice, while IL-17-producing cells were decreased by butyrate. The *in vitro* experiment showed similar results to the *in vivo* experiment; B10 cells and IL-17-producing cells were decreased and increased by butyrate. The numbers of $B220^{+}$- and $ROR\alpha^{+}$- cells in the salivary glands and expression levels of *RORα* increased in butyrate-treated mice compared to vehicle-treated mice. Also, the *RORα*-positive population increased in butyrate-treated cells compared to vehicle-treated cells. Of note, the effect of butyrate increasing IL-10 production was inhibited by treatment with the *RORα* antagonist, SR3335. In addition, B10 cells decreased in $ROR\alpha^{fl/fl}$/CD19-Cre mice compared to wild-type mice, and butyrate did not induce production of IL-10. In previous studies, butyrate was shown to regulate T cell function; However, our data imply that butyrate regulates not only T-cell but also B-cell function through regulation of *RORα*.

Circadian clock genes are related to salivary gland disorders such as SS [47]. *NR1D1*, a circadian-clock-related gene, regulates the differentiation of Th17 cells via the circadian-clock network [30]. In a previous study, we demonstrated the therapeutic effect of butyrate in an RA mouse model via *NR1D1*. In this study, we showed that numbers of *NR1D1*-positive cells and expression levels of *NR1D1* decreased in butyrate-treated mice and cells. Expression levels of *NFIL3*, which is negatively regulated by *NR1D1*, increased under *NR1D1* inhibition. As expected, expression levels of *NFIL3* increased in butyrate-treated cells. Treatment with butyrate resulted in a decrease in IL-17-producing B cells but did not affect the *NFIL3*-deleted condition. Butyrate regulates the immune response as a signaling molecule of GPCR [48] or an inhibitor of HDAC [49]. Our data reveal a new function of butyrate, namely, regulation of B cell function through regulation of circadian-clock-related genes.

In our study, a NOD mouse model was used to determine whether butyrate could alleviate SS, and it was confirmed that salivary flow rate and salivary gland tissue inflammation were regulated by butyrate (Figs. 1 and 2). In HSG cells, a human cell line related to SS, butyrate regulated cell death and circadian-clock-related genes (Fig. 3). B cells producing IL-10 and IL-17 were increased and decreased by butyrate, respectively (Figs. 4 and 5). B cell regulation of butyrate was confirmed to be through the circadian-clock-related genes *RORα* and *NR1D1* (Figs. 6 and 7). In summary, it was confirmed that butyrate regulates B cells in SS, and this is the first study to confirm that butyrate has the potential to treat SS.

SS is a systemic autoimmune disease that is characterized by infiltration of immune cells into salivary glands. The infiltration of immune cells, especially IL17-producing T cells, causes the destruction and dysfunction of tissue. In addition, metabolic abnormality exacerbates SS by increasing IL-17-producing cells in salivary glands [50]. Various immune cells play roles in the pathogenesis of RA. IL-17- and IL10-producing cells regulate collagen-induced arthritis through the IL-17/IL-10 balance by Th17 and Bregs [46].

In summary, our study has identified butyrate as a regulator for the development of SS. Butyrate alleviates the infiltration of immune cells into salivary glands and induces B10 cells. Our findings imply that butyrate may be a suitable candidate therapeutic target for SS.

Author statement

Da Som Kim: Conceptualization, Investigation, Methodology, Project administration, Software, Validation, Visualization, Writing - original draft, Writing - review & editing, Jin Seok Woo: Writing - original draft, Writing - review & editing, Hong-Ki Min: Writing - original draft, Jeong-Won Choi: Project administration, Jeong Hyeon Moon: Project administration, Min-Jung Park: Project administration, Seung-Ki Kwok: Funding acquisition, Supervision, Sung-Hwan Park: Conceptualization, Funding acquisition, Supervision, Mi-La Cho: Conceptualization, Funding acquisition, Supervision, Writing - review & editing.

Declaration of competing interest

There are no competing interests in relation to the work described.

Acknowledgments

This work was supported by the National Research Foundation of Korea (NRF) grant funded by the Korea government (MSIT) (No. 2020R1A2C2099615) and the Bio & Medical Technology Development Program of the National Research Foundation (NRF) & funded by the Korean government (MSIT) (No. NRF-2017M3A9F3041045).

Appendix A. Supplementary data

Supplementary data to this article can be found online at https://doi.org/10.1016/j.jaut.2021.102611.

References

[1] C.Q. Nguyen, H. Yin, B.H. Lee, W.C. Carcamo, J.A. Chiorini, A.B. Peck, Pathogenic effect of interleukin-17A in induction of Sjogren's syndrome-like disease using adenovirus-mediated gene transfer, Arthritis Res. Ther. 12 (2010) R220.
[2] M. Voulgarelis, A.G. Tzioufas, Pathogenetic mechanisms in the initiation and perpetuation of Sjogren's syndrome, Nat. Rev. Rheumatol. 6 (2010) 529–537.
[3] J. Moon, S.H. Choi, C.H. Yoon, M.K. Kim, Gut dysbiosis is prevailing in Sjogren's syndrome and is related to dry eye severity, PloS One 15 (2020), e0229029.
[4] C. Tsigalou, E. Stavropoulou, E. Bezirtzoglou, Current insights in microbiome shifts in sjogren's syndrome and possible therapeutic interventions, Front. Immunol. 9 (2018) 1106.
[5] C.S. de Paiva, D.B. Jones, M.E. Stern, F. Bian, Q.L. Moore, S. Corbiere, et al., Altered mucosal microbiome diversity and disease severity in sjogren syndrome, Sci. Rep. 6 (2016) 23561.
[6] A. Barcenilla, S.E. Pryde, J.C. Martin, S.H. Duncan, C.S. Stewart, C. Henderson, et al., Phylogenetic relationships of butyrate-producing bacteria from the human gut, Appl. Environ. Microbiol. 66 (2000) 1654–1661.
[7] R. Kant, P. Rasinkangas, R. Satokari, T.E. Pietila, A. Palva, Genome sequence of the butyrate-producing anaerobic bacterium Anaerostipes hadrus PEL 85, Genome Announc. (2015) 3.
[8] I. Lagkouvardos, R. Pukall, B. Abt, B.U. Foesel, J.P. Meier-Kolthoff, N. Kumar, et al., The Mouse Intestinal Bacterial Collection (miBC) provides host-specific insight

into cultured diversity and functional potential of the gut microbiota, Nat Microbiol 1 (2016) 16131.
[9] H. Liu, C. Hou, G. Wang, H. Jia, H. Yu, X. Zeng, et al., Lactobacillus reuteri I5007 modulates intestinal host defense peptide expression in the model of IPEC-J2 cells and neonatal piglets, Nutrients 9 (2017).
[10] C. Belzer, L.W. Chia, S. Aalvink, B. Chamlagain, V. Piironen, J. Knol, et al., Microbial metabolic networks at the mucus layer lead to diet-independent butyrate and vitamin B12 production by intestinal symbionts, mBio 8 (2017).
[11] Y. Ritze, G. Bardos, A. Claus, V. Ehrmann, I. Bergheim, A. Schwiertz, et al., Lactobacillus rhamnosus GG protects against non-alcoholic fatty liver disease in mice, PloS One 9 (2014), e80169.
[12] Y. Furusawa, Y. Obata, S. Fukuda, T.A. Endo, G. Nakato, D. Takahashi, et al., Commensal microbe-derived butyrate induces the differentiation of colonic regulatory T cells, Nature 504 (2013) 446–450.
[13] N.D. Mathewson, R. Jenq, A.V. Mathew, M. Koenigsknecht, A. Hanash, T. Toubai, et al., Gut microbiome-derived metabolites modulate intestinal epithelial cell damage and mitigate graft-versus-host disease, Nat. Immunol. 17 (2016) 505–513.
[14] M. Mizuno, D. Noto, N. Kaga, A. Chiba, S. Miyake, The dual role of short fatty acid chains in the pathogenesis of autoimmune disease models, PloS One 12 (2017), e0173032.
[15] W. Hui, D. Yu, Z. Cao, X. Zhao, Butyrate inhibit collagen-induced arthritis via Treg/IL-10/Th17 axis, Int. Immunopharm. 68 (2019) 226–233.
[16] M. Kim, Y. Qie, J. Park, C.H. Kim, Gut microbial metabolites fuel host antibody responses, Cell Host Microbe 20 (2016) 202–214.
[17] H.N. Sanchez, J.B. Moroney, H. Gan, T. Shen, J.L. Im, T. Li, et al., B cell-intrinsic epigenetic modulation of antibody responses by dietary fiber-derived short-chain fatty acids, Nat. Commun. 11 (2020) 60.
[18] H.Y. Liao, L. Tao, J. Zhao, J. Qin, G.C. Zeng, S.W. Cai, et al., Clostridium butyricum in combination with specific immunotherapy converts antigen-specific B cells to regulatory B cells in asthmatic patients, Sci. Rep. 6 (2016) 20481.
[19] Y. Shi, L.Z. Xu, K. Peng, W. Wu, R. Wu, Z.Q. Liu, et al., Specific immunotherapy in combination with Clostridium butyricum inhibits allergic inflammation in the mouse intestine, Sci. Rep. 5 (2015) 17651.
[20] M. Luu, S. Pautz, V. Kohl, R. Singh, R. Romero, S. Lucas, et al., The short-chain fatty acid pentanoate suppresses autoimmunity by modulating the metabolic-epigenetic crosstalk in lymphocytes, Nat. Commun. 10 (2019) 760.
[21] D.S. Kim, J.E. Kwon, S.H. Lee, E.K. Kim, J.G. Ryu, K.A. Jung, et al., Attenuation of rheumatoid inflammation by sodium butyrate through reciprocal targeting of HDAC2 in osteoclasts and HDAC8 in T cells, Front. Immunol. 9 (2018) 1525.
[22] J. Mielle, R. Audo, M. Hahne, L. Macia, B. Combe, J. Morel, et al., IL-10 producing B cells ability to induce regulatory T cells is maintained in rheumatoid arthritis, Front. Immunol. 9 (2018) 961.
[23] K. Yanaba, J.D. Bouaziz, T. Matsushita, T. Tsubata, T.F. Tedder, The development and function of regulatory B cells expressing IL-10 (B10 cells) requires antigen receptor diversity and TLR signals, J. Immunol. 182 (2009) 7459–7472.
[24] A. Mizoguchi, A.K. Bhan, A case for regulatory B cells, J. Immunol. 176 (2006) 705–710.
[25] P.M. Schlegel, I. Steiert, I. Kotter, C.A. Muller, B cells contribute to heterogeneity of IL-17 producing cells in rheumatoid arthritis and healthy controls, PloS One 8 (2013), e82580.
[26] A. Vazquez-Tello, R. Halwani, R. Li, J. Nadigel, A. Bar-Or, B.D. Mazer, et al., IL-17A and IL-17F expression in B lymphocytes, Int. Arch. Allergy Immunol. 157 (2012) 406–416.
[27] L. Zhou, S. Peng, J. Duan, J. Zhou, L. Wang, J. Wang, A human B cell line AF10 expressing HIL-17, Biochem. Mol. Biol. Int. 45 (1998) 1113–1119.
[28] D.A. Bermejo, S.W. Jackson, M. Gorosito-Serran, E.V. Acosta-Rodriguez, M. C. Amezcua-Vesely, B.D. Sather, et al., Trypanosoma cruzi trans-sialidase initiates a program independent of the transcription factors RORgammat and Ahr that leads to IL-17 production by activated B cells, Nat. Immunol. 14 (2013) 514–522.
[29] P.K.M. Oliveira-Brito, M.C. Roque-Barreira, T.A. da Silva, The response of IL-17-producing B cells to ArtinM is independent of its interaction with TLR2 and CD14, Molecules 23 (2018).
[30] X. Yu, D. Rollins, K.A. Ruhn, J.J. Stubblefield, C.B. Green, M. Kashiwada, et al., TH17 cell differentiation is regulated by the circadian clock, Science 342 (2013) 727–730.
[31] M.F. Farez, I.D. Mascanfroni, S.P. Mendez-Huergo, A. Yeste, G. Murugaiyan, L. P. Garo, et al., Melatonin contributes to the seasonality of multiple sclerosis relapses, Cell 162 (2015) 1338–1352.
[32] T. Kobayashi, K. Matsuoka, S.Z. Sheikh, H.Z. Elloumi, N. Kamada, T. Hisamatsu, et al., NFIL3 is a regulator of IL-12 p40 in macrophages and mucosal immunity, J. Immunol. 186 (2011) 4649–4655.
[33] Q. Cao, X. Zhao, J. Bai, S. Gery, H. Sun, D.C. Lin, et al., Circadian clock cryptochrome proteins regulate autoimmunity, Proc. Natl. Acad. Sci. U. S. A. 114 (2017) 12548–12553.
[34] D. Druzd, O. Matveeva, L. Ince, U. Harrison, W. He, C. Schmal, et al., Lymphocyte circadian clocks control lymph node trafficking and adaptive immune responses, Immunity 46 (2017) 120–132.
[35] C. Dawes, Circadian rhythms in human salivary flow rate and composition, J. Physiol. 220 (1972) 529–545.
[36] V. Leone, S.M. Gibbons, K. Martinez, A.L. Hutchison, E.Y. Huang, C.M. Cham, et al., Effects of diurnal variation of gut microbes and high-fat feeding on host circadian clock function and metabolism, Cell Host Microbe 17 (2015) 681–689.
[37] J.L. Kaczmarek, S.M. Musaad, H.D. Holscher, Time of day and eating behaviors are associated with the composition and function of the human gastrointestinal microbiota, Am. J. Clin. Nutr. 106 (2017) 1220–1231.
[38] J.A. Deaver, S.Y. Eum, M. Toborek, Circadian disruption changes gut microbiome taxa and functional gene composition, Front. Microbiol. 9 (2018) 737.
[39] Y. Tahara, M. Yamazaki, H. Sukigara, H. Motohashi, H. Sasaki, H. Miyakawa, et al., Gut microbiota-derived short chain fatty acids induce circadian clock entrainment in mouse peripheral tissue, Sci. Rep. 8 (2018) 1395.
[40] G.J. Shim, M. Warner, H.J. Kim, S. Andersson, L. Liu, J. Ekman, et al., Aromatase-deficient mice spontaneously develop a lymphoproliferative autoimmune disease resembling Sjogren's syndrome, Proc. Natl. Acad. Sci. U. S. A. 101 (2004) 12628–12633.
[41] S. Pringle, L.S.Y. Nanduri, v. d. Z. Marianne, v. O. Ronald, R.P. Coppes, Isolation of mouse salivary gland stem cells, J. Vis. Exp. 48 (2011) e2484.
[42] K. Yanagi, N. Ishimaru, N. Haneji, K. Saegusa, I. Saito, Y. Hayashi, Anti-120-kDa alpha-fodrin immune response with Th1-cytokine profile in the NOD mouse model of Sjogren's syndrome, Eur. J. Immunol. 28 (1998) 3336–3345.
[43] M. Polihronis, N.I. Tapinos, S.E. Theocharis, A. Economou, C. Kittas, H. M. Moutsopoulos, Modes of epithelial cell death and repair in Sjogren's syndrome (SS), Clin. Exp. Immunol. 114 (1998) 485–490.
[44] Y. Onishi, HSG cells, a model in the submandibular clock, Biosci. Rep. 31 (2011) 57–62.
[45] K. Kodukula, D.V. Faller, D.N. Harpp, I. Kanara, J. Pernokas, M. Pernokas, et al., Gut microbiota and salivary Diagnostics: the mouth is salivating to tell us something, Biores Open Access 6 (2017) 123–132.
[46] J. Jhun, H.K. Min, J. Ryu, S.Y. Lee, J.G. Ryu, J.W. Choi, et al., Lactobacillus sakei suppresses collagen-induced arthritis and modulates the differentiation of T helper 17 cells and regulatory B cells, J. Transl. Med. 18 (2020) 317.
[47] S. Papagerakis, L. Zheng, S. Schnell, M.A. Sartor, E. Somers, W. Marder, et al., The circadian clock in oral health and diseases, J. Dent. Res. 93 (2014) 27–35.
[48] P.V. Chang, L. Hao, S. Offermanns, R. Medzhitov, The microbial metabolite butyrate regulates intestinal macrophage function via histone deacetylase inhibition, Proc. Natl. Acad. Sci. U. S. A. 111 (2014) 2247–2252.
[49] J.M. Blouin, G. Penot, M. Collinet, M. Nacfer, C. Forest, P. Laurent-Puig, et al., Butyrate elicits a metabolic switch in human colon cancer cells by targeting the pyruvate dehydrogenase complex, Int. J. Canc. 128 (2011) 2591–2601.
[50] S.H. Hwang, J.S. Park, S. Yang, K.A. Jung, J. Choi, S.K. Kwok, et al., Metabolic abnormalities exacerbate Sjogren's syndrome by and is associated with increased the population of interleukin-17-producing cells in NOD/ShiLtJ mice, J. Transl. Med. 18 (2020) 186.